ACADEMIC PRESS

Available online at www.sciencedirect.com
SCIENCE DIRECT®

Journal of Sound and Vibration 261 (2003) 1–15

JOURNAL OF SOUND AND VIBRATION

www.elsevier.com/locate/jsvi

Boundary element analysis of packed silencers with protective cloth and embedded thin surfaces

T.W. Wu[a,*], C.Y.R. Cheng[b], Z. Tao[a]

[a] *Department of Mechanical Engineering, University of Kentucky, 521 CRMS Building, Lexington, KY 40506-0503, USA*
[b] *Nelson Industries, Inc., Stoughton, WI 53589, USA*

Received 8 October 2001; accepted 5 April 2002

Abstract

Bulk-reacting porous materials are often used as absorptive lining in packed silencers to reduce broadband noise. Modelling the entire silencer domain with a bulk-reacting material will inevitably involve two different acoustic media, air and the bulk-reacting material. A so-called direct mixed-body boundary element method (BEM) has recently been developed to model the two-medium problem in a single-domain fashion. The present paper is an extension of the direct mixed-body BEM to include protective cloth and embedded rigid surfaces. Protective cloth, an absorptive material itself with a higher flow resistivity than the primary lining material, is usually sandwiched between a perforated metal surface and the lining to protect the lining material from any abrasive effect of the grazing flow. Two different approaches are taken to model the protective cloth. One is to approximate sound pressure as a linear function across the cloth thickness and then use the bulk-reacting material properties of the cloth to obtain the transfer impedance. The other is to measure the transfer impedance of the cloth directly by an experimental set-up similar to the two-cavity method. As for an embedded thin surface, it is a rigid thin surface sandwiched between two bulk-reacting linings. Numerical modelling of an embedded thin surface is similar to the modelling of a rigid thin surface in air. Several test cases are given and the BEM results for transmission loss (TL) are verified by experimental TL measurements.

1. Introduction

Silencers used in industry usually contain very complex internal components such as extended inlet/outlet tubes, thin baffles, perforated tubes, and bulk-reacting sound absorbing materials.

*Corresponding author. Tel.: +1-859-257-2662; fax: +1-859-257-3304.
E-mail address: timwu@engr.uky.edu (T.W. Wu).

0022-460X/03/$ - see front matter
PII: S0022-460X(02)00897-0

Although the interior fluid domain is bounded, the boundary element method (BEM) is still an ideal analysis tool due to its surface-only meshing scheme. A so-called "direct mixed-body BEM" has been developed to model mufflers with rigid internal thin components and perforated tubes [1,2]. The method has recently been extended to packed silencers with bulk-reacting lining [3]. In the context of the direct mixed-body BEM, each surface component has its own attribute. Fig. 1 shows a typical packed silencer that can be modelled by the direct mixed-body BEM. With reference to the figure, the symbols R, T, P, B, I, IP and ATB stand for "Regular", "Thin", "Perforated", "Bulk reacting", "Interface", "Interface with Perforated tube", and "Air–Thin–Bulk reacting" surfaces respectively. The R surfaces include the exterior silencer surfaces (with no bulk-reacting packing), the external inlet/outlet tubes, and the inlet/outlet ends. The T surfaces are the thin components inside the silencer, such as the extended inlet/outlet tubes, thin baffles, thin flow plugs, and internal connecting tubes. The P surfaces are designated for perforated surfaces with air on both sides. The B surfaces are the exterior boundary surfaces with the bulk-reacting material. The I surfaces are the interfaces between the bulk-reacting material and air. The IP surfaces are the perforated interfaces between the bulk-reacting material and air. The ATB surfaces represent any rigid thin plates between the bulk-reacting material and air.

Traditionally, the two-medium problem as depicted in Fig. 1 would have required a multi-domain approach with each subdomain homogeneous [4] if the BEM is to be used. However, it is very tedious to define each subdomain and to match the interface boundary conditions between different subdomains, especially when the subdomains are connected to one another in a complicated way. Sometimes imaginary interfaces may have to be used when thin components are involved [5]. The multi-domain BEM has also been used for mufflers with perforated tubes [6,7]. The direct mixed-body BEM totally eliminates the tedious multi-domain approach by simply summing up all the subdomain integral equations. Hypersingular normal-derivative integral equations are used on certain surfaces to provide additional equations when pressure and normal velocity are both unknowns there. As such, a multi-domain problem can be implemented in a single-domain fashion, even though there are two different acoustic media involved. In addition, in the direct mixed-body BEM, a silencer model can be easily created by assembling different surface components together, thanks to the use of constant elements. Each surface component is assigned a surface type (such as R, T, P, B, I, etc.) when the component is created. The mesh of each component is then automatically refined at each frequency step of calculation. That means a

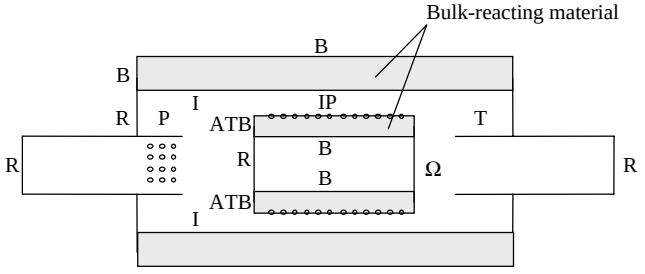

Fig. 1. Types of surfaces modelled in the direct mixed-body BEM (no fluid outside the silencer).

very coarse mesh is used at low frequencies, and the mesh is automatically refined as frequency goes up.

The concept of the direct-mixed body BEM is not totally against the traditional multi-domain BEM, though. For a very large problem, a substructuring technique [8] may still be needed to break a large structure into smaller substructures, to save CPU time and memory space. However, with the direct mixed-body BEM, each substructure may contain very complex internal components and bulk-reacting linings. As a result, substructuring can be done naturally along the silencer longitudinal direction. The traditional multi-domain rule of having to construct homogeneous (single-medium) and well defined (no thin or perforated surfaces) subdomains is no longer required.

This paper is an extension of the direct mixed-body BEM to include two more kinds of surfaces commonly used in packed silencers. The first kind of surface to be included is a layer of protective cloth sandwiched between a perforated surface and a bulk-reacting lining. Protective cloth, a sound-absorbing material itself with a higher flow resistivity than the lining material, is usually wrapped around a perforated tube before the bulk-reacting lining outside the perforated tube is packed. Because the thickness of the cloth is so small, modelling the layer as a third acoustic domain in the BEM is not a practical approach. A lumped transfer impedance relating the sound pressure difference across the layer thickness to the normal velocity of the layer has been used in some analytical modelling methods [9–11]. For an impermeable layer, the transfer impedance is a product function of frequency, mass density, and layer thickness [10,11]. For a thin, limp resistive scrim, the transfer impedance also depends on flow resistivity [11]. In this paper, two different methods are used to obtain the transfer impedance of the protective cloth. The first method assumes a linear variation of sound pressure across the thickness of the cloth and uses that approximation in the acoustic momentum equation. This results in the same transfer impedance formula as in the case of an impermeable layer, although the protective cloth is not really impermeable. However, the density is now defined as the bulk-reacting density (a complex number) measured by the two-cavity method [12], instead of the conventional mass density for an impermeable layer. The second method is to measure the transfer impedance of the cloth directly by an experimental set-up similar to the two-cavity method. The measurement is actually simpler than the two-cavity method because the cavity size does not need to be changed. It is noted that no flow effect is considered in this study for simplicity. Once the transfer impedance of the cloth is obtained by either method, it is combined with the transfer impedance of the perforated tube. The combined transfer impedance is then used in the BEM. The surface type designated for this kind of surface is interface with perforated tube and cloth (IPC) in the direct mixed-body BEM.

The second type of surface to be included is a rigid thin surface embedded in a bulk-reacting material or sandwiched between two bulk-reacting lining of the same kind. The surface type is referred to as bulk reacting–thin–bulk reacting (BTB). The BEM modelling of BTB is similar to the method for thin surfaces in air (T). The hypersingular integral equation is used and the pressure jump is the primary unknown variable associated with BTB.

Adding these two new types of surfaces, IPC and BTB, to the direct mixed-body boundary integral equations results in a more complete set of boundary integral equations for silencer analysis. Several test cases are presented to verify the formulation. Transmission loss (TL) is evaluated in each test case. The BEM predictions for TL are compared to the experimental TL measurements.

2. Transfer impedance at IPC interface

As shown in Fig. 2, a thin layer of cloth with thickness h is sandwiched between a bulk-reacting lining and a perforated surface. The cloth itself is a bulk-reacting material with a higher flow resistivity than the main lining material that it protects. In the direct mixed-body BEM, the combined cloth and perforated metal surface forms the so-called IPC interface between air and the bulk-reacting lining. Let ρ_A, ρ_B, ρ_C, c_A, c_B, and c_C denote the mean densities and speeds of sound of air, bulk-reacting lining, and cloth respectively. Note that ρ_B, ρ_C, c_B, and c_C are all complex numbers and can be measured by the two-cavity method [12]. Also, let p_A, p_B, p_C denote the sound pressures at the three different locations shown in Fig. 2. Define a normal direction that points into the air side. We begin with the acoustic momentum equation in the cloth layer,

$$-\frac{\partial p}{\partial n} = \mathrm{i}\rho_C \omega v_n, \tag{1}$$

where $\mathrm{i} = \sqrt{-1}$, ω is the angular frequency, and v_n is the normal particle velocity. Because the thickness of the cloth is very small, it is assumed that the normal particle velocity is constant across the thickness and the sound pressure has a linear variation. Eq. (1) then becomes

$$\frac{p_B - p_C}{h} = \mathrm{i}\rho_C \omega v_n. \tag{2}$$

In other words, the transfer impedance of the cloth can be represented by

$$\frac{p_B - p_C}{v_n} = \mathrm{i}\rho_C \omega h. \tag{3}$$

Eq. (3) is identical to the transfer impedance formula given for an impermeable membrane [10,11], although the cloth is not really impermeable. The difference here is that the mean density in Eq. (3) is the bulk-reacting density measured from the two-cavity method, instead of the mass density, to account for the porous sound absorbing effects of cloth.

Also, with reference to Fig. 2, the transfer impedance across the perforated metal surface is

$$\frac{p_C - p_A}{v_n} = \rho_A c_A \xi, \tag{4}$$

where ξ is the dimensionless transfer impedance for the perforated surface. At room temperature and in the absence of mean flow, a simple empirical formula given by Sullivan and Crocker [13] in

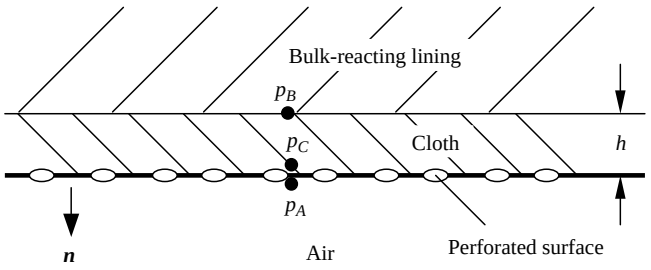

Fig. 2. IPC interface.

the linear regime is

$$\xi = \frac{1}{\rho_A c_A \sigma}(2.4 + \mathrm{i}0.02f), \tag{5}$$

where f is the frequency in Hz, and σ is the porosity (the open to the total area ratio). Note that the two constants 2.4 and 0.02 are in MKS units. Alternative empirical formulas that use additional parameters such as wall thickness, hole diameter, and Mach number are also available [14,15] and have been used in BEM modelling [2].

Add Eq. (3) to Eq. (4) to eliminate p_C, and the transfer impedance for the IPC interface is

$$\frac{p_B - p_A}{v_n} = \rho_A c_A \xi + \mathrm{i}\rho_C \omega h. \tag{6}$$

Eq. (6) can then be used in direct mixed-body BEM formulation. The IPC integral formulation will be identical to the IP integral formulation [3] if the following modified dimensionless transfer impedance ξ^* is used:

$$\xi^* = \begin{cases} \xi & \text{on IP,} \\ \xi + \mathrm{i}\rho_C \omega h/(\rho_A c_A) & \text{on IPC.} \end{cases} \tag{7}$$

3. Transfer impedance measurement

One potential problem in using Eq. (7) is that it is difficult to measure the cloth thickness precisely due to the small thickness and the deformable nature of cloth. Different persons may come up with very different thickness values using exactly the same measurement tool and the same piece of cloth sample. That means Eq. (7) will have to be expressed in the area density form ($\rho_C h$ lumped into a single variable called "area density"). In other words, the thickness value used in the BEM modelling has to be the same as the thickness value used in the two-cavity measurement for a particular piece of cloth. As long as the same thickness value is used, the thickness value itself does not need to be very precise. However, this also means that the bulk-reacting density ρ_C measured from a particular piece of cloth is hardly a material property and cannot be applied to another piece of cloth with a different thickness value.

An alternative way is to measure the transfer impedance of cloth directly. Fig. 3 illustrates the experimental setup for such a direct measurement using an impedance tube. The setup actually is

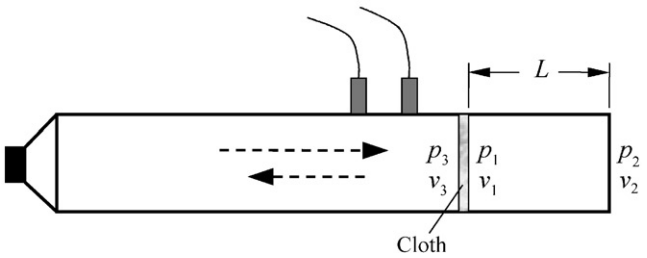

Fig. 3. Transfer impedance measurement.

very similar to the two-cavity method except that the back cavity length L does not need to be changed. Let p_1, p_2, and p_3 denote the sound pressures, and v_1, v_2, and v_3 denote the particle velocities in the positive axis direction at the three different locations shown in Fig. 3 respectively. Because the cloth is very thin, a single particle velocity v is assumed across the cloth thickness, i.e., $v = v_3 = v_1$. First, the local impedance of the combined cloth and back cavity is measured by the two-microphone method [16]. This produces a local impedance z_3 defined by $z_3 = p_3/v$. Next, the four-pole matrix for the back cavity is written as

$$\begin{bmatrix} p_1 \\ v_1 \end{bmatrix} = \begin{bmatrix} \cos k_A L & \mathrm{i}\rho_A c_A \sin k_A L \\ \dfrac{\mathrm{i}}{\rho_A c_A} \sin k_A L & \cos k_A L \end{bmatrix} \begin{bmatrix} p_2 \\ v_2 \end{bmatrix}, \tag{8}$$

where k_A is the wavenumber in air. Since $v_2 = 0$ due to the rigid end condition, the local impedance z_1 due to the back cavity only is

$$z_1 = \frac{p_1}{v} = \frac{\cos k_A L}{(\mathrm{i}/\rho_A c_A) \sin k_A L} = -\mathrm{i}\rho_A c_A \cot k_A L, \tag{9}$$

provided that L is selected such that $\sin k_A L \neq 0$ in the measured frequency range. The transfer impedance of the cloth is then the difference between z_3 (measured by the two-microphone method) and z_1 (calculated by Eq. (9)). That is,

$$\frac{p_3 - p_1}{v} = z_3 - z_1. \tag{10}$$

When this transfer impedance for cloth is applied to the IPC configuration in Fig. 2, the modified dimensionless transfer impedance ξ^* defined in Eq. (7) becomes

$$\xi^* = \begin{cases} \xi & \text{on IP,} \\ \xi + (z_3 - z_1)/(\rho_A c_A) & \text{on IPC.} \end{cases} \tag{11}$$

4. Direct mixed-body BEM

The concept of the direct mixed-body BEM actually begins with the conventional multi-domain BEM by subdividing the acoustic domain into several homogeneous and well-defined subdomains. The Helmholtz integral equation can be written for each individual subdomain. All the subdomain integral equations are then summed up to produce one single integral equation. The normal-derivative hypersingular integral equation is used to provide an additional equation at any interfaces that have two unknown variables.

The procedure can be demonstrated by a simplified two-medium problem as shown in Fig. 4. Let Ω_A denote the air subdomain, and Ω_B the bulk-reacting material subdomain. The interface between the two subdomains is an IPC interface. Let $\mathbf{n}$ be the unit normal vector. The unit normal vector on R or B boundary is pointing into the interior acoustic domain, and on the IPC interface the normal is pointing into the air side. Let p_A and p_B denote the sound pressure in air and the bulk-reacting material respectively. If the $e^{+i\omega t}$ convention is adopted, the Helmholtz integral

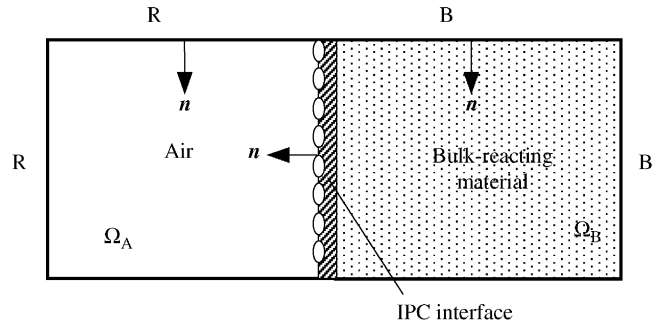

Fig. 4. Two-medium problem.

equations for two individual subdomains are

$$\int_R \left(p_A \frac{\partial \psi_A}{\partial n} + \mathrm{i}\rho_A \omega v_n \psi_A \right) \mathrm{d}S + \int_{IPC} \left(p_A \frac{\partial \psi_A}{\partial n} + \mathrm{i}\rho_A \omega v_n \psi_A \right) \mathrm{d}S$$

$$= \begin{cases} 4\pi p_A(P), & P \in \Omega_A, \quad (12a) \\ 2\pi p_A(P), & P \in R + IPC, \quad (12b) \\ 0, & P \in \Omega_B + B, \quad (12c) \end{cases}$$

$$\int_B \left(p_B \frac{\partial \psi_B}{\partial n} + \mathrm{i}\rho_B \omega v_n \psi_B \right) \mathrm{d}S - \int_{IPC} \left(p_B \frac{\partial \psi_B}{\partial n} + \mathrm{i}\rho_B \omega v_n \psi_B \right) \mathrm{d}S$$

$$= \begin{cases} 4\pi p_B(P), & P \in \Omega_B, \quad (13a) \\ 2\pi p_B(P), & P \in B + IPC, \quad (13b) \\ 0, & P \in \Omega_A + R, \quad (13c) \end{cases}$$

where P is the collocation point, ψ_A and ψ_B are the free-space Green functions in air and the bulk-reacting material respectively. A negative sign is used in front of the integral over IPC in Eq. (13) because the normal at the IPC interface is pointing into air. Due to the use of constant elements, the solid angle at P on the surface is always 2π. The explicit expressions for the two Green functions are

$$\psi_A = \frac{\mathrm{e}^{-\mathrm{i}k_A r}}{r}, \quad (14a)$$

$$\psi_B = \frac{\mathrm{e}^{-\mathrm{i}k_B r}}{r}, \quad (14b)$$

where k_A and k_B are the wavenumbers in air and the bulk-reacting material, respectively, $r = |P - Q|$, and Q is any integration point on the boundary. At the IPC interface, the jump condition is

$$p_B = p_A + \rho_A c_A \xi^* v_n, \quad (15)$$

where ξ^* is the modified dimensionless transfer impedance given in Eq. (7) or (11). Substitute Eq. (15) into Eq. (13) on the IPC surface and then sum up Eqs. (12) and (13). This

produces

$$\int_R \left(p \frac{\partial \psi_A}{\partial n} + \mathrm{i}\rho_A \omega v_n \psi_A \right) \mathrm{d}S + \int_B \left(p \frac{\partial \psi_B}{\partial n} + \mathrm{i}\rho_B \omega v_n \psi_B \right) \mathrm{d}S + \int_{IPC} \left[p_A \left(\frac{\partial \psi_A}{\partial n} - \frac{\partial \psi_B}{\partial n} \right) - \rho_A c_A \xi^* v_n \frac{\partial \psi_B}{\partial n} + \mathrm{i}\omega v_n (\rho_A \psi_A - \rho_B \psi_B) \right] \mathrm{d}S = \begin{cases} 4\pi p(P), & P \in \Omega_A + \Omega_B, \quad (16a) \\ 2\pi p(P), & P \in R + B, \quad (16b) \\ 4\pi p_A(P) + 2\pi \rho_A c_A \xi^* v_n(P), & P \in IPC, \quad (16c) \end{cases}$$

where the subscript (A or B) for sound pressure p on R and B as well as in the domains is omitted because the definition of a unique p is clear there.

Since there are two unknowns at each node on IPC, Eq. (16c) needs a companion normal-derivative hypersingular integral equation. That is,

$$\int_R \left(p \frac{\partial^2 \psi_A}{\partial n \partial n^P} + \mathrm{i}\rho_A \omega v_n \frac{\partial \psi_A}{\partial n^P} \right) \mathrm{d}S + \int_B \left(p \frac{\partial^2 \psi_B}{\partial n \partial n^P} + \mathrm{i}\rho_B \omega v_n \frac{\partial \psi_B}{\partial n^P} \right) \mathrm{d}S + \int_{IPC} \left[p_A \left(\frac{\partial^2 \psi_A}{\partial n \partial n^P} - \frac{\partial^2 \psi_B}{\partial n \partial n^P} \right) - \rho_A c_A \xi^* v_n \frac{\partial^2 \psi_B}{\partial n \partial n^P} + \mathrm{i}\omega v_n \left(\rho_A \frac{\partial \psi_A}{\partial n^P} - \rho_B \frac{\partial \psi_B}{\partial n^P} \right) \right] \mathrm{d}S = -2\pi \mathrm{i}\omega (\rho_A + \rho_B) v_n(P), \quad P \in IPC. \quad (17)$$

The integral formulation for BTB is similar to the thin-body integral formulation in air (T), which can be found in Ref. [1]. Basically, a normal direction can be pointing into either side of the rigid thin surface. The pressure on the side that the normal is pointing into is denoted by p^+, while pressure on the opposite side is denoted by p^-. The detailed derivation is omitted here. One advantage of the direct mixed-body BEM is that adding new surface types is straightforward. With the addition of IPC and BTB, the complete boundary integral equations become

$$\int_R \left(p \frac{\partial \psi_A}{\partial n} + \mathrm{i}\rho_A \omega v_n \psi_A \right) \mathrm{d}S + \int_{T+\mathrm{P}} \frac{\partial \psi_A}{\partial n} (p^+ - p^-) \, \mathrm{d}S + \int_{BTB} \frac{\partial \psi_B}{\partial n} (p^+ - p^-) \, \mathrm{d}S + \int_B \left(p \frac{\partial \psi_B}{\partial n} + \mathrm{i}\rho_B \omega v_n \psi_B \right) \mathrm{d}S + \int_I \left[p \left(\frac{\partial \psi_A}{\partial n} - \frac{\partial \psi_B}{\partial n} \right) + \mathrm{i}\omega v_n (\rho_A \psi_A - \rho_B \psi_B) \right] \mathrm{d}S + \int_{IP+IPC} \left[p_A \left(\frac{\partial \psi_A}{\partial n} - \frac{\partial \psi_B}{\partial n} \right) - \rho_A c_A \xi^* v_n \frac{\partial \psi_B}{\partial n} + \mathrm{i}\omega v_n (\rho_A \psi_A - \rho_B \psi_B) \right] \mathrm{d}S + \int_{ATB} \left(p_A \frac{\partial \psi_A}{\partial n} - p_B \frac{\partial \psi_B}{\partial n} \right) \mathrm{d}S = \begin{cases} 4\pi p(P), & P \in \Omega, \quad (18a) \\ 2\pi p(P), & P \in R + B, \quad (18b) \\ 2\pi [p^+(P) + p^-(P)], & P \in T + \mathrm{P} + BTB, \quad (18c) \\ 4\pi p(P), & P \in I, \quad (18d) \\ 4\pi p_A(P) + 2\pi \rho_A c_A \xi^* v_n(P), & P \in IP + IPC, \quad (18e) \\ 2\pi [p_A(P) + p_B(P)], & P \in ATB, \quad (18f) \end{cases}$$

and

$$\int_R \left(p \frac{\partial^2 \psi_A}{\partial n \partial n^P} + \mathrm{i}\rho_A \omega v_n \frac{\partial \psi_A}{\partial n^P} \right) \mathrm{d}S + \int_{T+\mathrm{P}} \frac{\partial^2 \psi_A}{\partial n \partial n^P} (p^+ - p^-)\, \mathrm{d}S$$
$$+ \int_{BTB} \frac{\partial^2 \psi_B}{\partial n \partial n^P} (p^+ - p^-)\, \mathrm{d}S + \int_B \left(p \frac{\partial^2 \psi_B}{\partial n \partial n^P} + \mathrm{i}\rho_B \omega v_n \frac{\partial \psi_B}{\partial n^P} \right) \mathrm{d}S$$
$$+ \int_I \left[p \left(\frac{\partial^2 \psi_A}{\partial n \partial n^P} - \frac{\partial^2 \psi_B}{\partial n \partial n^P} \right) + \mathrm{i}\omega v_n \left(\rho_A \frac{\partial \psi_A}{\partial n^P} - \rho_B \frac{\partial \psi_B}{\partial n^P} \right) \right] \mathrm{d}S$$
$$+ \int_{IP+IPC} \left[p_A \left(\frac{\partial^2 \psi_A}{\partial n \partial n^P} - \frac{\partial^2 \psi_B}{\partial n \partial n^P} \right) - \rho_A c_A \xi^* v_n \frac{\partial^2 \psi_B}{\partial n \partial n^P} + \mathrm{i}\omega v_n \left(\rho_A \frac{\partial \psi_A}{\partial n^P} - \rho_B \frac{\partial \psi_B}{\partial n^P} \right) \right] \mathrm{d}S$$
$$+ \int_{ATB} \left(p_A \frac{\partial^2 \psi_A}{\partial n \partial n^P} - p_B \frac{\partial^2 \psi_B}{\partial n \partial n^P} \right) \mathrm{d}S$$
$$= \begin{cases} 0, & P \in T + BTB + ATB, \quad (19a) \\ 4\pi \dfrac{\mathrm{i}k_A}{\xi} [p^+(P) - p^-(P)], & P \in \mathrm{P}, \quad (19b) \\ -2\pi \mathrm{i}\omega(\rho_A + \rho_B) v_n(P). & P \in I + IP + IPC, \quad (19c) \end{cases}$$

5. Test cases

Several test models were constructed to verify the BEM results. An experimental TL measurement was carried out for each test model to provide a benchmark solution. The first test model was a fully packed expansion chamber. The dimensions of the packed expansion chamber are shown in Fig. 5. The bulk-reacting lining used was polyester, which has a flow resistivity of 16 000 MKS rayl/m. First, the model was tested without having any perforated tubes or cloth. Therefore, the interface between the bulk-reacting material and air was classified as an I surface. Fig. 6 shows the comparison between the BEM predicted TL values and the experimental TL curve. It is seen that the BEM results compare very well with the experiment. From the figure, it is also seen that the packed silencer provides very high absorption as the frequency increases.

Then a perforated tube was added to the test model to create an IP interface between air and the bulk-reacting lining. The configuration is shown in Fig. 7. The porosity of the perforated tube is

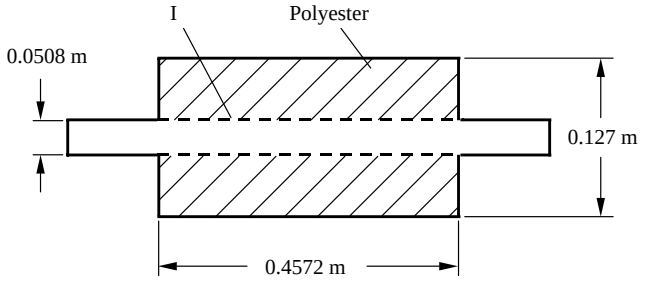

Fig. 5. Fully packed expansion chamber.

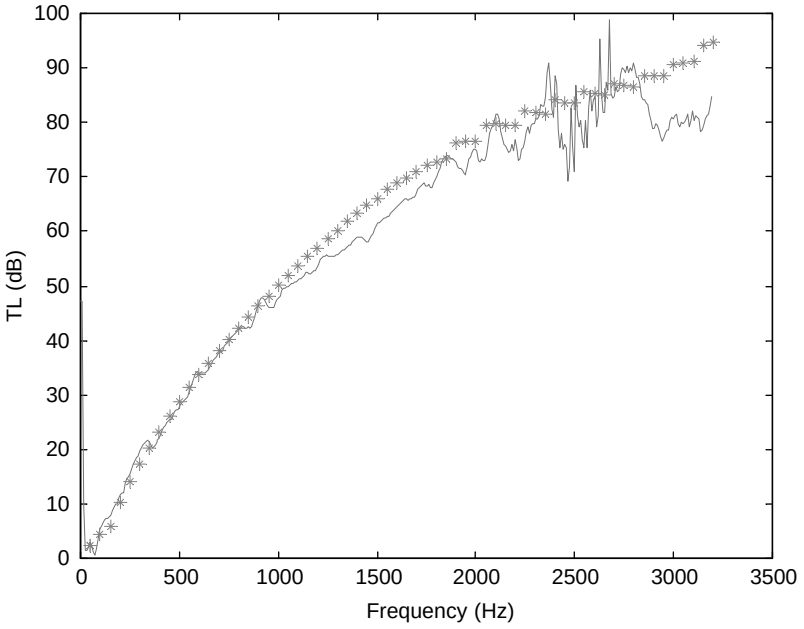

Fig. 6. TL for the fully packed expansion chamber in Fig. 5: —, experiment; ∗, BEM prediction.

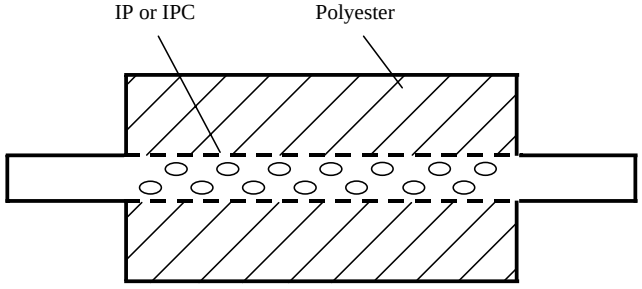

Fig. 7. Fully packed expansion chamber with a perforated tube, and with/without cloth.

19.6%; the thickness of the tube surface is 0.0012 m, and the diameter of each hole is 0.003175 m. The comparison between the BEM results and the experimental data is shown in Fig. 8. It is observed that after around 2200 Hz, the TL begins to drop a little, although the overall absorption effect is still quite high.

To test the IPC modelling, the perforated tube was wrapped by a layer of fiberglass cloth, which has a flow resistivity of 360 000 MKS rayl/m, before the polyester was packed (Fig. 7). The thickness of the cloth is around 2.54×10^{-4} m, which is only an estimate. Two separate BEM runs were carried out. The first BEM run used the mean density and thickness (Eq. (7)) to evaluate the transfer impedance; the second BEM run used the measured transfer impedance (Eq. (11)) directly. These two different approaches actually produced very similar TL results. The comparison between the BEM results and the experimental TL curve is shown in Fig. 9. From

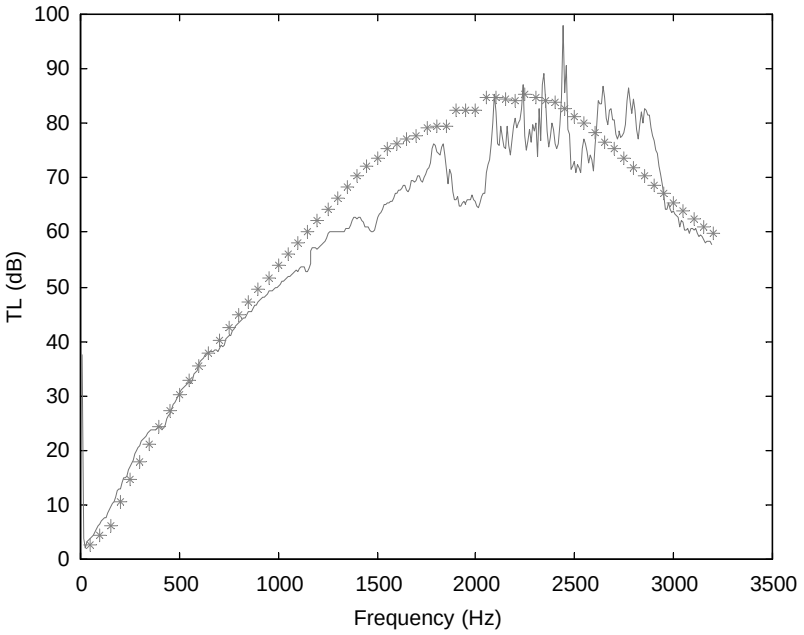

Fig. 8. TL for the fully packed expansion chamber in Fig. 7 with an IP interface: —, experiment; ∗, BEM prediction.

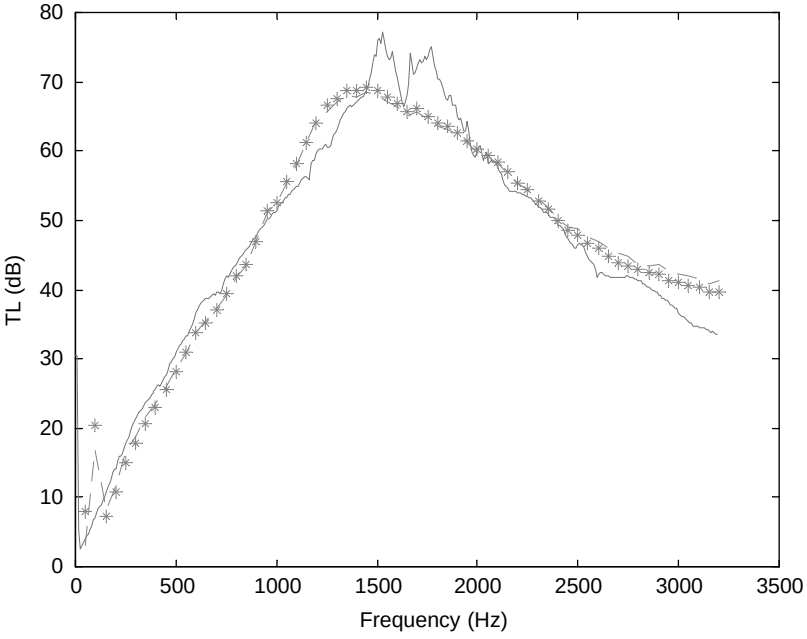

Fig. 9. TL for the fully packed expansion chamber in Fig. 7 with an IPC interface: —, experiment; ∗, BEM prediction using Eq. (7); - - -, BEM prediction using Eq. (11).

the figure, it is observed that the TL starts to decline at around 1500 Hz. That means the high flow resistivity of the protective cloth does have some negative effect on sound absorption.

A center rigid baffle was then added to the model. Only the front half of the chamber was packed with polyester. As such, the center baffle is classified as an ATB surface. The perforated tube was kept in the model. The model was tested with and without the fiberglass cloth, as shown in Fig. 10. Figs. 11 and 12 show the comparison between the BEM results and the experimental measurements for the test model with and without the cloth respectively. Very good agreement is observed in each case.

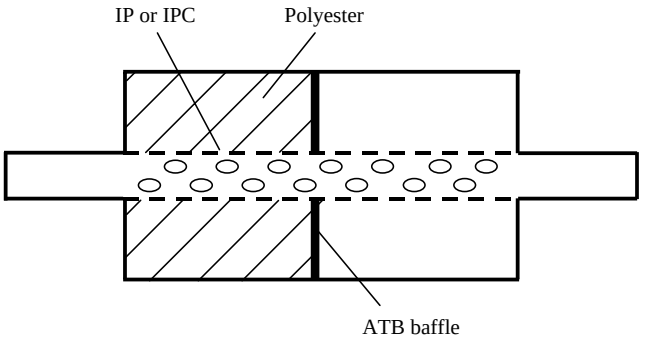

Fig. 10. Half-packed expansion chamber with a center baffle, a perforated tube, and with/without cloth.

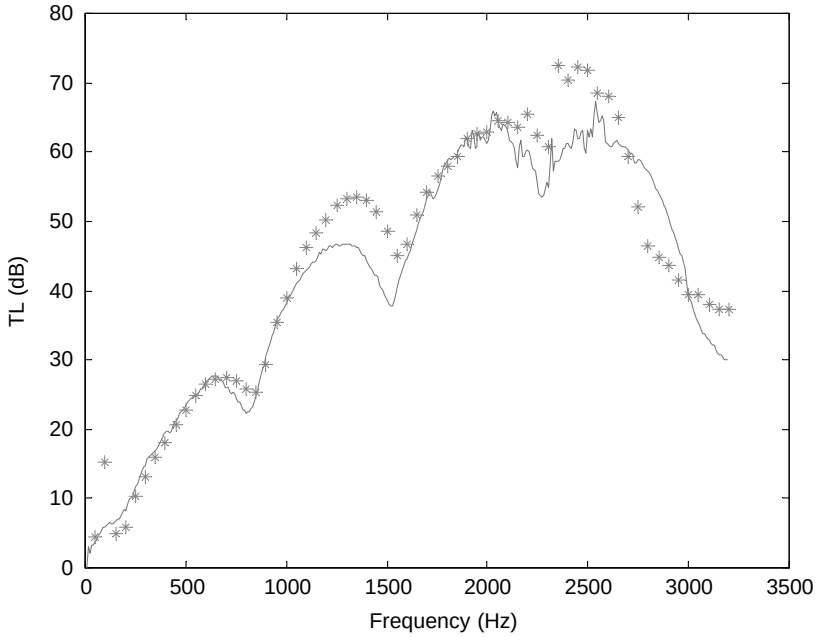

Fig. 11. TL for the half-packed expansion chamber in Fig. 10 with an IP interface: —, experiment; ∗, BEM prediction.

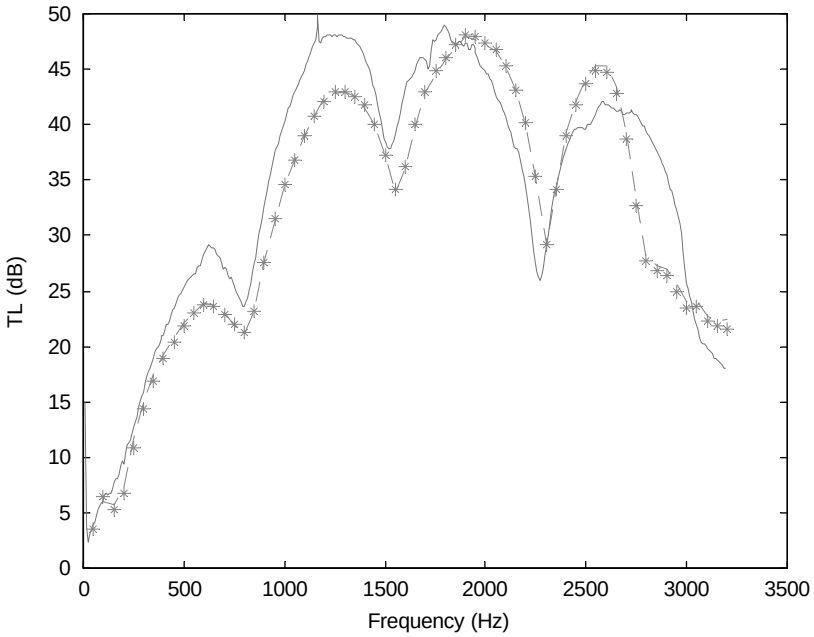

Fig. 12. TL for the half-packed expansion chamber in Fig. 10 with an IPC interface: —, experiment; ∗, BEM prediction using Eq. (7); - - -, BEM prediction using Eq. (11).

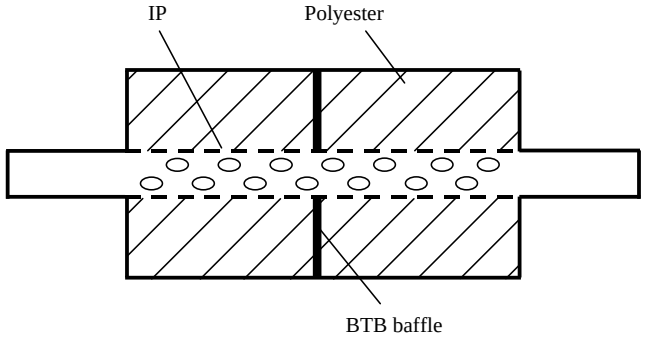

Fig. 13. Fully packed expansion chamber with a center baffle (BTB), a perforated tube, and no cloth (IP interface).

Finally, the second half of the chamber was also packed with polyester. This produced a BTB test case, as shown in Fig. 13. The center baffle becomes a BTB surface when both sides are packed. Since the focus of this last test case was on BTB, no cloth was used in this test case for simplicity. The comparison between the BEM prediction and the experimental TL curve is shown in Fig. 14. Again, very good agreement is observed.

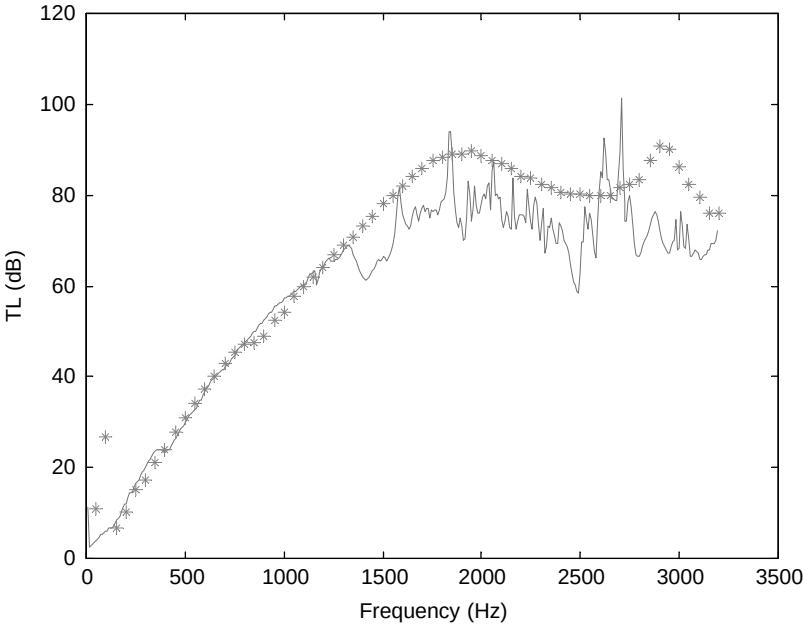

Fig. 14. TL for the BTB test case in Fig. 13: —, experiment; ∗, BEM prediction.

6. Conclusions

The direct mixed-body BEM for silencer analysis is expanded in this paper to include two new types of surfaces, IPC and BTB. The transfer impedance of the protective cloth is modelled by two approaches. The first approach uses the bulk-reacting mean density and thickness of the cloth to produce the transfer impedance. The second approach measures the transfer impedance directly. Both approaches are actually very similar and have produced almost identical results. The direct measurement of transfer impedance seems easier to use because there is no need to input the thickness. Also, the bulk-reacting mean density of the cloth is somewhat misleading because its value is based on (and very sensitive to) the not-so-accurate thickness. Although the BEM results will still be good if the same thickness as in the two-cavity measurement is used, the mean density has lost its role as a material property.

Derivation of the direct mixed-body boundary integral equations is demonstrated on a simple two-medium configuration with an IPC interface. The complete integral equations for silencer analysis are provided in this paper. Several test cases including IPC and BTB surfaces have been carried out. The BEM results compare very well with the experimental TL measurements.

No flow effect is considered in this study. Although the mean flow may not have a significant effect on the acoustic equations, it may have some effects on the transfer impedance of cloth. It is well known that flow does have effects on the transfer impedance of perforated tubes [15]. Future study should include the flow effect on the IPC interface in the BEM modelling.

Acknowledgements

This research was supported by Nelson Industries, Inc. Z. Tao was supported by Vibro-Acoustics Consortium at the University of Kentucky. The authors would also like to thank Dr. A.F. Seybert for providing laboratory space and equipment to complete some of the measurements.

References

[1] T.W. Wu, G.C. Wan, Muffler performance studies using a direct mixed-body boundary element method and a three-point method for evaluating transmission loss, Journal of Vibration and Acoustics, American Society of Mechanical Engineers Transactions 118 (1996) 479–484.
[2] T.W. Wu, P. Zhang, C.Y.R. Cheng, Boundary element analysis of mufflers with an improved method for deriving the four-pole parameters, Journal of Sound and Vibration 217 (1998) 767–779.
[3] T.W. Wu, C.Y.R. Cheng, P. Zhang, A direct mixed-body boundary element method for packed silencers, Journal of the Acoustical Society of America 111 (2002) 2566–2572.
[4] H. Utsuno, T.W. Wu, A.F. Seybert, T. Tanaka, Prediction of sound fields in cavities with sound absorbing materials, American Institute of Aeronautics and Astronomy Journal 28 (1990) 1870–1876.
[5] C.Y.R. Cheng, A.F. Seybert, T.W. Wu, A multidomain boundary element solution for silencer and muffler performance prediction, Journal of Sound and Vibration 151 (1991) 119–129.
[6] Z.H. Jia, A.R. Mohanty, A.F. Seybert, Numerical modeling of reactive perforated mufflers, in: M.J. Crocker, P.K. Raju (Eds.), Proceedings of the Second International Congress on Recent Developments in Air- and Structure-Borne Sound and Vibration, Auburn University, 1992, pp. 957–964.
[7] C.N. Wang, C.C. Tse, Y.N. Chen, A boundary element analysis of a concentric-tube resonator, Engineering Analysis with Boundary Elements 12 (1993) 21–27.
[8] Z. Ji, Q. Ma, Z. Zhang, Application of the boundary element method to predicting acoustic performance of expansion chamber mufflers with mean flow, Journal of Sound and Vibration 173 (1994) 57–71.
[9] Y. Minkin, A. Ginesin, Mathematical model of high pressure drop silencers with layered parallel baffles, in: R.J. Bernhard, J.S. Bolton (Eds.), Proceedings of the INTER-NOISE '95, Newport Beach, CA, 1995, pp. 465–468.
[10] M.L. Munjal, P.T. Thawani, Effect of protective layer on performance of absorptive ducts, Noise Control Engineering Journal 45 (1997) 14–18.
[11] H.-Y. Lai, S. Katragadda, J.S. Bolton, J.H. Alexander, Layered fibrous treatments for sound absorption and sound transmission, SAE Paper No. 972064, 1997, pp. 1553–1560.
[12] H. Utsuno, T. Tanaka, T. Fujikawa, A.F. Seybert, Transfer function method for measuring characteristic impedance and propagation constant of porous materials, Journal of the Acoustical Society of America 86 (1989) 637–643.
[13] J.W. Sullivan, M.J. Crocker, Analysis of concentric-tube resonators having unpartitioned cavities, Journal of the Acoustical Society of America 64 (1978) 207–215.
[14] M.L. Munjal, Acoustics of Ducts and Mufflers, Wiley-Interscience, New York, 1987.
[15] K.N. Rao, M.L. Munjal, Experimental evaluation of impedance of perforates with grazing flow, Journal of Sound and Vibration 108 (1986) 283–295.
[16] A.F. Seybert, D.F. Ross, Experimental determination of acoustic properties using a two-microphone random-excitation technique, Journal of the Acoustical Society of America 61 (1977) 1362–1370.